

Holocene peat and lake sediment tephra record from the southernmost Chilean Andes (53-55°S)

Rolf Kilian

Department of Geology, FB VI, University Trier,
54286 Trier, Germany
kilian@uni-trier.de

Miriam Hohner

Department of Geology, University of Freiburg, Albertstr. 23B,
79140 Freiburg, Germany

Harald Biester

Institute of Environmental Geochemistry, University of Heidelberg, INF 236,
69120 Heidelberg, Germany

Hans J. Wallrabe-Adams

Marum, University of Bremen, Klagenfurter Straße,
D-28359 Bremen, Germany

Charles R. Stern

Department of Geological Sciences, University of Colorado,
Boulder, Colorado 80309-0399 U.S.A.

ABSTRACT

Peat and lake sediment cores from Peninsula Muñoz Gamero in the southernmost Main Andean Cordillera, and also Seno Skyring fjord and Peninsula Brunswick in the Andean foothills, have been investigated to refine the local Holocene tephrochronology. New ^{14}C ages, together with calculated peat growth and sedimentation rates, provide age constraints. The thickest (5-15 cm) tephra layer in the cores resulted from an eruption of the Mount Burney volcano at approximately 4254 ± 120 cal. yr BP. Isopach maps for this eruption indicate deposition of approximately $2.5\text{--}3 \text{ km}^3$ of tephra, mainly in the forested Andean area southeast of the volcano. Mount Burney had another large Plinian eruption between 9009 ± 17 and 9175 ± 111 cal. yr BP, and also four smaller eruptions during the Holocene. Tephra from large explosive eruptions of the Reclus ($>15384 \pm 578$ cal. yr BP), Hudson (between 7707 ± 185 and 7795 ± 131 cal. yr BP) and Aguilera ($<3596 \pm 230$ cal. yr BP) volcanoes also occur in some of the cores as indicated by the characteristic compositions of their tephra glass, which differ both from each other and also from that of tephra derived from Mount Burney. Significant loss of alkali elements during alteration of the volcanic glass in the tephra layers was observed, especially within acid peat soils, and this may be an important factor in the plant nutrient supply.

Key words: Volcanism, Holocene, Tephra, Cordillera de los Andes, Mount Burney, Patagonia.

RESUMEN

El registro de tefras australes holocenas en turbas y sedimentos lacustres de los Andes meridionales (53-55°S), Chile. Se han estudiado testigos de tefras y sedimentos de la península Muñoz Gamero con el seno Skyring y con el propósito de mejorar la tefrocronología local. Nuevas edades ^{14}C junto con tasas de crecimiento de las turbas y de sedimentación, proporcionan nuevas marcas para la edad de las tefras. La capa más gruesa de tefra (5-15

cm) se originó en una erupción del volcán del monte Burney, a los $4,254 \pm 120$ años calibrados AP. Las isópachas de esta erupción indican una deposición de ca. 2,5 a 3 km³ de tefra, principalmente en el área andina forestada, al sureste del volcán. El monte Burney tuvo otra gran erupción pliniana entre $9,009 \pm 17$ y $9,175 \pm 110$ años cal. AP, y cuatro erupciones menores durante el Holoceno. Se observan, también, en algunos testigos tefras de las grandes erupciones de los volcanes Reclus ($>15,384 \pm 578$ cal. años AP), Hudson (entre $7,707 \pm 185$ y $7,795 \pm 131$ cal. años AP) y Aguilera ($<3,596 \pm 230$ cal. años AP) como lo indican las composiciones características de los vidrios de tefra, los cuales difieren entre los diferentes centros volcánicos. Se estableció una pérdida significativa de los elementos alcalinos durante la alteración del vidrio volcánico en las capas de tefra, especialmente en los testigos de suelos ácidos, lo que podría ser un factor importante en el suministro de nutrientes para las plantas.

Palabras claves: Volcanismo, Tefra, Holoceno, Cordillera de los Andes, Monte Burney, Patagonia.

INTRODUCTION

Tephra layers represent important time markers within peat and lake sediment cores, which are studied to reconstruct paleoclimate and paleo-environment (Markgraf, 1993; Heusser, 1995, 1998; Heusser *et al.*, 1989, 1990; McCulloch *et al.*, 2000; Markgraf *et al.*, 2003). Stratigraphic correlations between different core sites often depend on the quality of determined tephra ages. For the tephra produced by large Holocene Plinian eruptions of the volcanic centers in the southernmost Andes (Fig. 1a), more precise dating also adds to our understanding of the frequency of explosive eruptions in this part of the Andean volcanic arc, potential regional volcanic hazards, and the possible role of these eruptions in producing global effects such as SO₂ peaks in Antarctic ice cores (*e.g.*, Steig *et al.*, 2000; Cole-Dai *et al.*, 2000).

The first tephrochronology of the southern Andes and southernmost Patagonia was presented by Auer (1965, 1974), Sahlstein (1932), and Salmi (1941). Later, it was refined by Stern (1990, 1991, 1992, 2000), who used the petrochemical and isotopic characteristics of tephra both as a correlation tool and to determine the volcanic centers from which specific tephra layers were derived. For the Magallanes and Tierra del Fuego area of southernmost Patagonia, Stern (1992, 2000) described five regionally distributed Late Pleistocene to Holocene tephra layers erupted from the Mount Burney, Reclus, Aguilera and Hudson volcanoes. The age

and general spatial distribution ($>$ trace isopach) of these five tephra layers are shown in figure 1a. With exception of the Hudson volcano (Naranjo and Stern 1998), more detailed tephra isopach maps for large eruptions of these volcanoes remain undetermined, in part because earlier studies were restricted to the subandean and Pampean areas to the east of the Main Andean Cordillera.

Here the authors focus on peat-bog and lake sediment cores from the region of the Main Andean Cordillera on Peninsula Muñoz Gamero (Fig. 1), where tephra were deposited on *Notofagus* forest and peatland (*e.g.*, Young, 1972). New ¹⁴C ages, together with calculated peat accumulation and sedimentation rates, provide a precise basis for dating of tephra layers. Since the active volcanoes of the Andean Austral Volcanic Zone, as well as the Hudson volcano of the Southern Volcanic Zone, are chemically distinct from each other (Stern 1990, 1991, 1992; Stern and Kilian 1996; Naranjo and Stern 1998), the sources of tephra layers may be determined by the major and trace element composition of their volcanic glass. Using chronologic and chemical data to correlate tephra layers from both cores and outcrops in Magallanes and Tierra del Fuego, the distribution and eruption volume of a large mid-Holocene plinian eruption of the Mount Burney volcano, at approximately 4254 ± 120 cal. yr BP (Fig. 1a), has been determined by mapping its tephra isopachs.

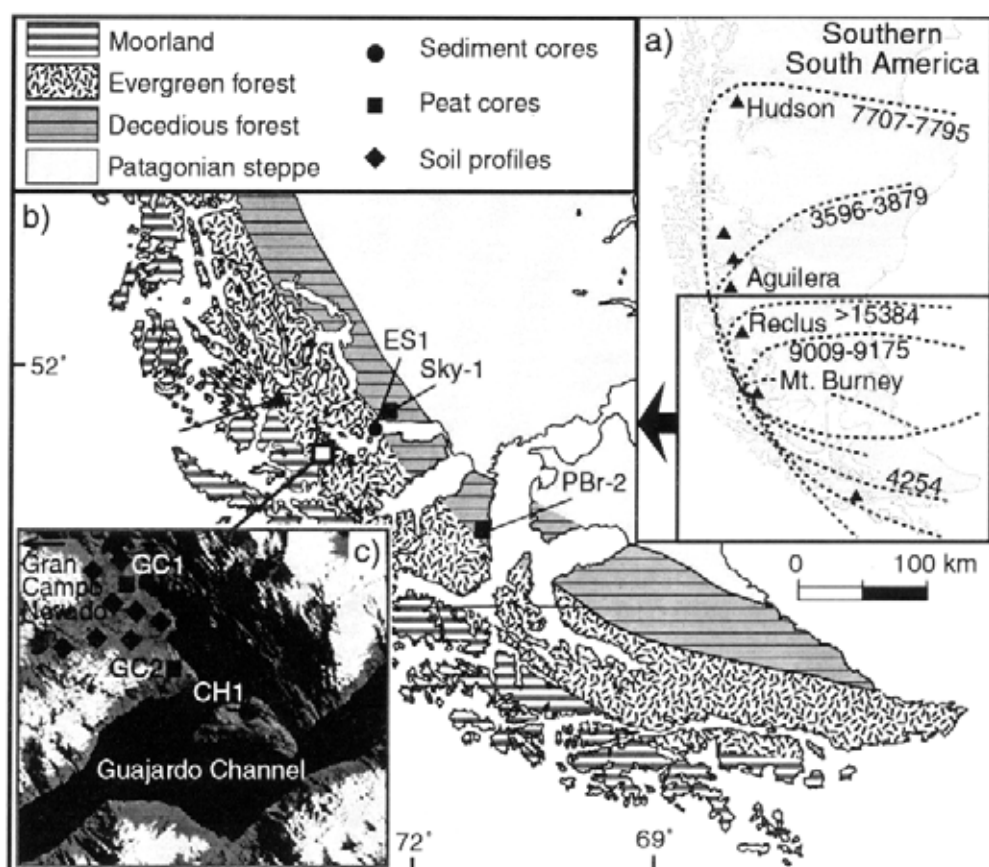


FIG. 1. Map of southernmost South America showing (a) the location of the volcanoes that have had Late Pleistocene and Holocene explosive eruptions, and the tephra fans (>trace isopach), modified to include the new results presented in this paper, produced by these eruptions (Stern 1990, 1991, 1992, 2000; Naranjo and Stern 1998); (b) the locations of peat and sediment cores discussed in this paper; and (c) a more detailed map of the locations of those cores taken from near the Gran Campo Nevado ice cap on Peninsula Muñoz Gamero. Also illustrated in (b) are the major vegetation zones, striking parallel to the Andean Cordillera (Markgraf, 1993).

SAMPLING AND ANALYTICAL TECHNIQUES

Peat cores were taken by a 2 m long stainless steel WARDENAAR corer with a serrated cutting edge which allows cutting through the roots of bog plants. Core sections deeper than 2 m were sampled with a Russian corer. Sediment cores were taken by 2 and 5 m long piston corers.

For the determination of the 'ash' content of peat cores, which indicates the amount of mineral matter in the peat calculated as weight per cent, 2 to 3 grams of sample were first freeze-dried and then dry-ashed for 4 hours at 550°C. This ash determination does include aeolian dust and tephra as well.

^{14}C measurements were done by a HVEE Tandem-tron accelerator mass spectrometry (AMS) at Leibniz Laboratory of the University of Kiel. The activity of ^{14}C was determined from acid extracts of terrestrial macrofossils. $^{13}\text{C}/^{12}\text{C}$ -ratios were measured simultaneously by AMS and used to correct mass fractionation. Conventional ^{14}C -ages were calibrated using CALIB rev4.3 data set 2 (Stuiver *et al.*, 1998). All reported ages (Table 1) are means of one-sigma values and the reported \pm values indicate the one-sigma range.

Mineral and glass major element chemistry of

the tephra (Table 2) was determined by electron microprobe (Cameca SX51; University of Heidelberg), equipped with five wave-length dispersive spectrometers, using an accelerating voltage of 15

kV and a beam current of 20 nA. The electron beam diameter was focused to $\sim 1 \mu\text{m}$ for most minerals, $\sim 5 \mu\text{m}$ for feldspar and 5–20 μm for glass. Natural and synthetic minerals were used for calibration.

SAMPLE LOCATIONS

To obtain a representative tephra record in the central part of the southernmost Main Andean Cordillera, the authors have taken two peat cores at Bahía Bahamondes (GC-1 and GC-2) and a sediment core from Lake Chandler (CH-1) as well as various soil profiles from Peninsula Muñoz Gamero near the Gran Campo Nevado ice cap (53°S ; Fig. 1c; Table 1). Rain-fed (ombrotrophic) peat sections, which represent peat solely fed through atmospheric deposition of nutrients were distinguished from ground water and run-off influenced minerogenic peats by their low Ca and Ti content and their lower pH (Biester *et al.*, 2003). At the Bahía Bahamondes near Gran Campo Nevado a mainly ombrogenic peat core (GC-1) represent a cushion plant bog built up dominantly by *Donatia fascicularis* and *Astelia pumilia*, and different *Carex* species with an average peat accumulation rate of 0.5 mm/year. The only other materials besides peat in this core were contributed by rain, air pollutants, aerosols, sea spray and volcanic tephra (Biester *et al.* 2002). Therefore, the mineral and glass content of this peat results essentially from tephra fall. The general weather situation in this Andean area (Schneider *et al.*, in press) precludes deposition of Patagonian pampa-derived fine dust. At an other locality of Bahía Bahamondees also a minerogenic peat (peat core GC-2; Fig. 1c) with peat accumulation rates of 0.1–0.3 mm/year was investigated. In addition to tephra and other atmospheric derived components, this peat also contains variable proportions of minerals and/or glass which were introduced as surface fluvial sediment, especially during the early stage of peat formation, which began in the Late Glacial. A 6.5 m long sediment core (CH-1; Fig. 1c) was also taken from a small 100-by-150 m lake Chandler. This small lake has a very restricted catchment area of moderate topography and only a few small tributaries. Organic-rich sediments (10–30% organic carbon) were deposited in the anoxic

lake bottom without bioturbation, so that even thin tephra layers, which are light-gray to yellow in color and easily visible in the dark-brown sediment core (Fig. 2), are very well preserved. Approximately 40

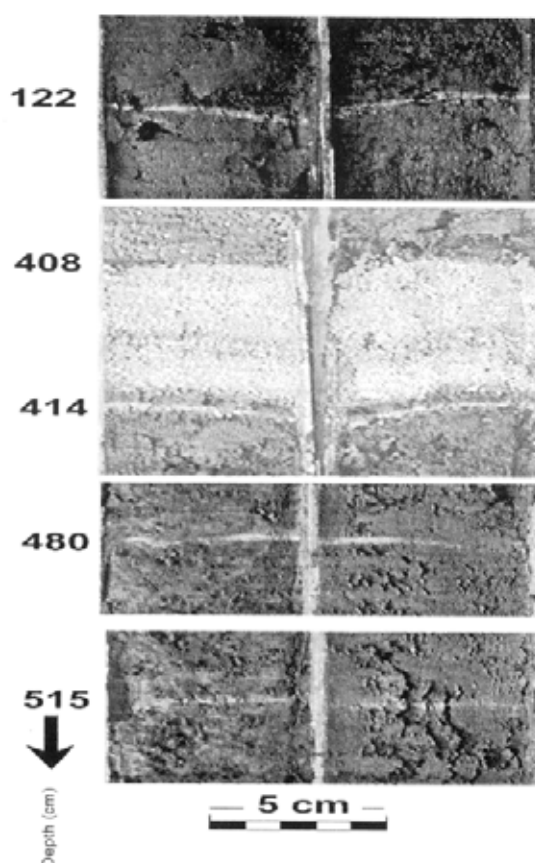


FIG. 2. Sections of the sediment core from lake Chandler on the Peninsula Muñoz Gamero (CH-1 in Fig. 1c), showing three tephra layers produced by eruptions of Mount Burney volcano between 2026 ± 48 to 2063 ± 90 cal. yr BP (122 cm core depth), at 4254 ± 120 cal. yr BP (408 and 414 cm), and between 9009 ± 17 to 9175 ± 111 cal. yr BP (515 cm). A further tephra layer is from the Hudson eruption at 7707 ± 185 to 7795 ± 131 cal. yr BP (480 cm).

TABLE 1. TEPHRA LAYERS (T) AND ACCELERATOR MASS SPECTROMETRY (AMS) ^{14}C AGES OF PEAT AND LAKE SEDIMENT PROFILES FROM PENINSULA MUÑOZ GAMERO, SENO SKYRING AND PENINSULA BRUNSWICK, MAGALLANES, CHILE.

Core	Location	Specification material	Dated corrected	Core depth	Percentage of Modern Carbon	$\delta^{13}\text{C}$	^{14}C age	Calibrated ages (yr $\pm 1\sigma$)	Calibrated yr BP (mean of 1σ)	Sedimentation/peat growth rates (mm/yr)
CH-1		Burney-T.		122.1-122.3						
CH-1	Isla Chandler	CHK1/5a-83-85	4.6 mg C	380 cm	84.52 \pm 0.24	-27.44 \pm 0.18‰	3520 \pm 30	3829, 3789, 3779, 3735	3879 (4254)	1.34
CH-1	Canal Gajardo			408-414 cm						
CH-1	Península									
CH-1	Muñoz	CHK1/5b-16-18	1.6 mg C	422 cm	57.70 \pm 0.29	-27.60 \pm 0.11‰	4420 \pm 40	5030, 5019, 4978	4961	
CH-1	Gamero	Hudson-T.		480-480.2 cm						
CH-1		Burney-T.		515.1-515.3 cm						
CH-1		CHK7/15-17	4.8 mg C	520 cm	36.31 \pm 0.20	-27.82 \pm 0.11‰	7890 \pm 45	9030	9175	0.23
CH-1		Burney-T.		524-524.2						
CH-1		CHK7/49-51	0.6 mg C	536 cm	34.61 \pm 0.32	-31.08 \pm 0.20‰	8520 \pm 70	9529	9511	0.28
CH-1		Burney-T.		557.3-537.5 cm						
CH-1		CHK7/85-86	2.9 mg C	605 cm	27.68 \pm 0.19	-28.20 \pm 0.11‰	10320 \pm 55	12595, 12509, 12352	12451	0.26
GC1	Bahía Bahamondes	GC1a 33	4.1 mg C	66 cm	82.71 \pm 0.36	-27.43 \pm 0.14‰	1529 \pm 28	1410	1409	
GC1	Canal Gajardo	GC1a-41	4.2 mg C	82 cm	78.58 \pm 0.33	-26.34 \pm 0.08‰	1944 \pm 29	1883	1879	0.34
GC1	Península	Tephra		85-105 cm						
GC1	Muñoz	GC1a-55	4.2 mg C	110 cm	76.25 \pm 0.33	-25.98 \pm 0.06‰	2169 \pm 28	2150	2213	
GC1	Gamero	GC1a 59	4.4 mg C	118 cm	74.26 \pm 0.52	-25.91 \pm 0.07‰	2421 \pm 31	2429, 2420, 2396, 2394, 2361	2416 (4254)	0.39
GC1		Burney-T		187-195						
GC2	Bahía Bahamondes									
GC2	Canal Gajardo	Burney-T.		38 cm						
GC2	(Fig. 1)	GC2-L1-30-32		42 cm	72.19 \pm 0.29	-27.77 \pm 0.06‰	2620 \pm 30	2650	2651	
GC2	Península	GC-2-25	2.1 mg C	44 cm	71.43 \pm 0.24	-26.75 \pm 0.08‰	2705 \pm 25	2758	2750	
GC2	Muñoz			50 cm	65.64 \pm 0.36	-27.77 \pm 0.07‰	3382 \pm 44	3621	3635 (4254)	
GC2	Gamero	Burney-T.		58-62 cm						
GC2		GC-2-58	4.0 mg C	116 cm	42.29 \pm 0.22	-25.76 \pm 0.10‰	6915 \pm 40	7723, 7707, 7702	7705	0.21
GC2		Hudson-T.		134 cm						
GC2		GC-2-72	2.2 mg C	144 cm	38.65 \pm 0.20	-26.70 \pm 0.09‰	7635 \pm 40	8409	8409	0.21
GC2		Burney-T.		150 cm						
GC2			4.3 mg C	195 cm	29.74 \pm 0.15	-29.23 \pm 0.05‰	9740 \pm 42	11174	11190	
GC2		GC2L2-269	0.3 mg C	269 cm	22.40 \pm 0.56	-31.95 \pm 0.07‰	12017 \pm 203	14072	14441	
Soil age			4.3 mg C	70 cm		-27.13 \pm 0.06‰	4719 \pm 49	5469	5453	

(table 1 continued)

Core	Location	Specification material	Dated corrected	Core depth	Percentage of modern carbon	$\delta^{13}\text{C}$	^{14}C age	Calibrated ages ($\text{yr} \pm 1\sigma$)	Calibrated yr BP (mean of 1σ)	Sedimentation/ peat grow rates (mm/yr)
Sky1	Northern Shore	Sky 17	3.6 mg C	68 cm	88.97 ± 0.43	$-28.34 \pm 0.24\text{‰}$	940 ± 40	910, 852, 834, 809, 799	858	0.79
Sky1	of Seno Skyring	Sky 30	4.1 mg C	120 cm	79.02 ± 0.26	$-27.77 \pm 0.12\text{‰}$	1892 ± 27	1860, 1851, 1824	1846	0.56
Sky1		Sky 42	3.7 mg C	168 cm	63.80 ± 0.27	$-27.64 \pm 0.12\text{‰}$	3610 ± 35	3900	3921 (4254)	0.28
Sky1		Burney-T. Sky 61	5.4 mg C	172-180 244 cm	29.74 ± 0.15	$-27.13 \pm 0.06\text{‰}$	5191 \pm xx	5952		0.33
Sky1		Burney-T.		275 cm						
Pbr2	Puerto del Hambre		5.8 mg C	70 cm	86.60 ± 0.32	$-26.89 \pm 0.10\text{‰}$	973 ± 29	923	865	
Pbr2	Peninsula		4.3 mg C	148 cm	81.83 ± 0.29	$-25.45 \pm 0.11\text{‰}$	1610 ± 30	1522	1481	1.25
Pbr2	Brunswick	Burney-T.		213-220 cm					(4254)	
Pbr2		Hudson-T.		308-310 cm						
Pbr2		Burney-T.		368-371 cm						
Pbr2			5.3 mg C	480 cm	30.50 ± 0.17	$-27.22 \pm 0.15\text{‰}$	9537 ± 46	11041, 11023, 10992, 10967, 10754	10893	0.35

Conventional ^{14}C -ages were calibrated using CALIB rev4.3 data set 2 (Stuiver et al., 1998). PMC= Percentage of Modern Carbon.

soil profiles, some reaching back to $>5454 \pm 136$ cal. yr BP (Table 1), have also been studied in the nearby area (Figs. 1c, 3).

In addition to the cores from the Main Andean Cordillera, a 4.2 m long clay-rich fjord sediment core (ES-1; Fig. 1b) was taken 3 km south of the northern shore of the proglacial lake Seno Skyring, near Escarpada Island, in a water depth of 80 m. Approximately 7 km northeast of this locality, a predominantly ombrogenic peat core was taken along the northern shore of Seno Skyring (Sky-1; Fig. 1b). Its peat accumulation rate increases from <0.2 mm/year in the lower core section to 0.4 mm/year in the upper part of the core (Fig. 4). In the lower

minerogetic clay-rich part of this core ($>5952 \pm 32$ cal. yr BP; Table 1), thin tephra layers are difficult or impossible to detect.

Another 6.5 m long peat core (Pbr-2; Fig. 1b) was taken near Puerto del Hambre along the northern shore of the Straits of Magellan on Peninsula Brunswick. Ombrogenic peat formation in this core reaches back continuously to 10883 ± 105 cal. yr BP (Fig. 4). Tephra identification in this core is much easier than in other partly minerogetic peat or sedimentary cores taken previously in the same area, such as the Puerto del Hambre peat core described by McCulloch and Davies (2001).

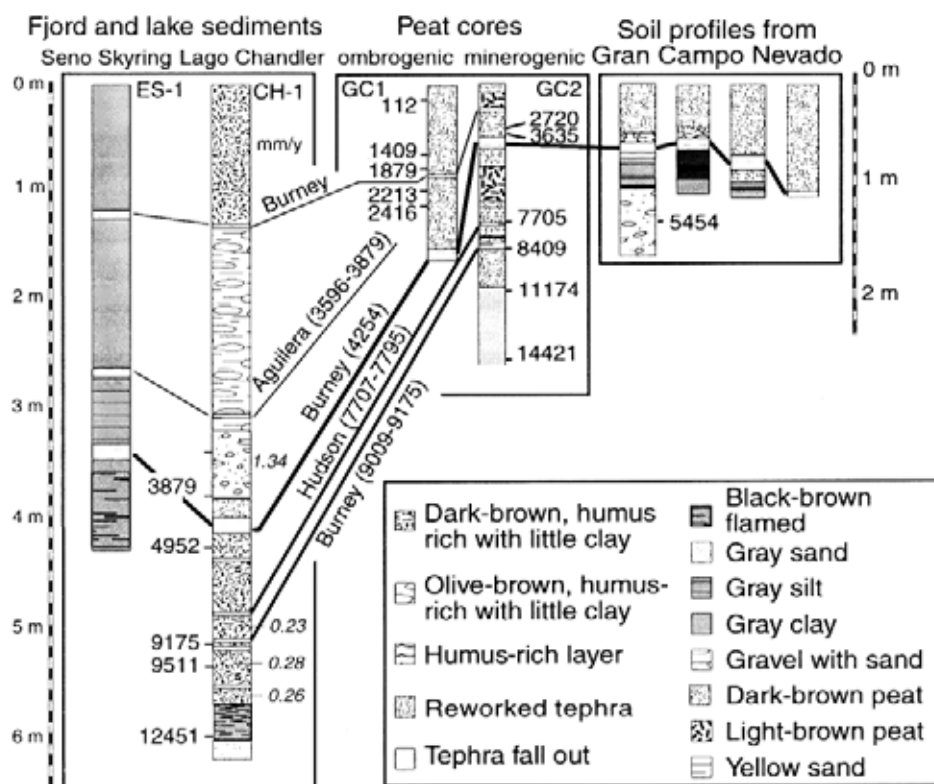


FIG. 3. Lithologic characteristics, stratigraphy and tephra layers of sediment, peat and soil profiles from Peninsula Muñoz Gamero and the northern shore of Seno Skyring (locations see Fig. 1a-c). From left to right: a sediment core from the northern shore of Seno Skyring (ES-1); a sediment core of Lake Chandler (CH-1) near the Gran Campo Nevado with sedimentation rates (mm/year; in italics; Table 1); an ombrogenic peat core (GC-1), a minerogetic peat core (GC-2) and soil profiles, all from the same area at Bahía Bahamondes near to the Gran Campo Nevado (Fig. 1c); Estimated minimum and maximum ages of tephra layers are given in cal. yr BP (details see discussion and Stern 1992, 2000).

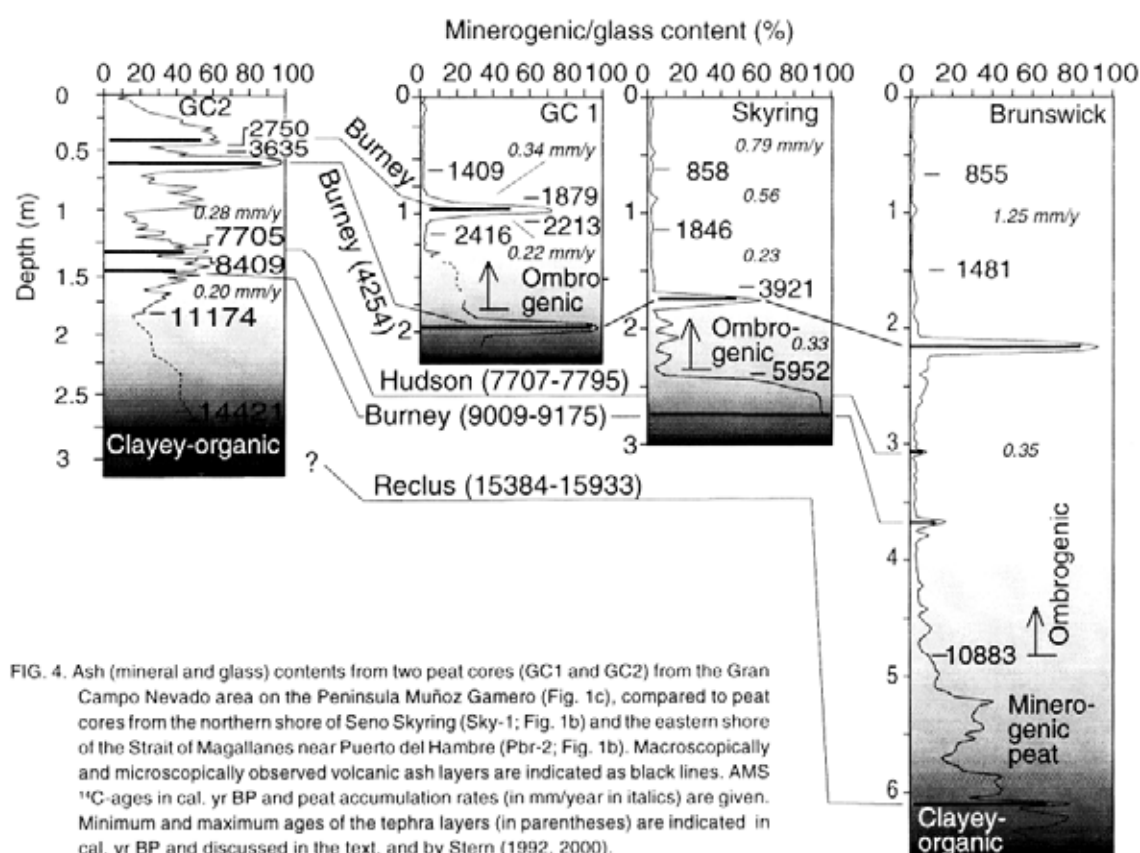


FIG. 4. Ash (mineral and glass) contents from two peat cores (GC1 and GC2) from the Gran Campo Nevado area on the Peninsula Muñoz Gamero (Fig. 1c), compared to peat cores from the northern shore of Seno Skyring (Sky-1; Fig. 1b) and the eastern shore of the Strait of Magallanes near Puerto del Hambre (Pbr-2; Fig. 1b). Macroscopically and microscopically observed volcanic ash layers are indicated as black lines. AMS ^{14}C -ages in cal. yr BP and peat accumulation rates (in mm/year in italics) are given. Minimum and maximum ages of the tephra layers (in parentheses) are indicated in cal. yr BP and discussed in the text, and by Stern (1992, 2000).

RESULTS AND DISCUSSION

TEPHRA PRESERVATION

Among the various peat and sediment cores, the organic-rich sediment core from the small lake Chandler (CH-1) on Peninsula Muñoz Gamero preserves the most tephra fall layers (Figs. 2-4). No root activity or bioturbation has disturbed small tephra fall layers in this lake. Furthermore, the light-gray tephra layers are easily visible in the dark-brown sediment core (Fig. 2). However extensive soil erosion and deposition in the lake, possibly due to plant destruction after the Mount Burney eruption of 4254 ± 120 cal. yr BP, makes radiocarbon dating in the upper part of the core difficult (Kilian *et al.*, 2001).

In contrast, thin tephra layers in peat cores are often dispersed by root growth after deposition. Therefore, fine-grained volcanic ash layers are often

difficult to detect and the original thickness of ashes is difficult to estimate in these cores. However, observation of the presence of very thin tephra layers was easier in ombrogenic peat cores than in minerogenic core sections. In the Late glacial minerogenic basal parts of the peat cores, the volcanic ash layers are particularly difficult to distinguish from fluvial-derived clayey sections in the peat. Ombrogenic peat formation started earlier in the area along the Strait of Magellan near the Puerto del Hambre site (after 10883 ± 105 cal. yr BP; Fig. 4) than along the north shore of Seno Skyring (after 5952 ± 32 cal. yr BP) or within the Andean Cordillera on Peninsula Muñoz Gamero ($>2420 \pm 70$ cal. yr BP; Blester *et al.*, 2002). This is due to ice-retreat, and also to postglacial uplift of shore lines, which both occurred progressively from east to west.

TABLE 2. CHEMICAL COMPOSITIONS, OF SELECTED VOLCANIC GLASS SAMPLES FROM DIFFERENT TEPHRA LAYERS IN THE SOUTHERNMOST ANDES.

Hudson					Reclus				
	Hu 4-9	Hu 4-10	Hu 4-11	Hu 4-12	Re 6-7	Re 6-13	Re 6-14	Re 6-15	Re 6-16
SiO ₂	76.22	79.29	77.51	78.24	79.13	79.52	78.83	79.49	76.76
TiO ₂	0.19	0.15	0.18	0.16	0.19	0.14	0.10	0.15	0.22
Al ₂ O ₃	13.74	11.82	13.63	13.88	13.07	12.94	12.94	12.46	13.12
Cr ₂ O ₃	0.04	0.00	0.00	0.00	0.00	0.00	0.00	0.04	0.00
FeO	1.16	0.88	1.10	1.10	1.35	1.23	1.24	1.24	1.61
MnO	0.02	0.02	0.02	0.00	0.07	0.05	0.03	0.08	0.05
MgO	0.16	0.18	0.14	0.18	0.21	0.18	0.24	0.22	0.26
CaO	1.19	1.07	1.19	1.05	1.53	1.58	1.42	1.43	2.23
Na ₂ O	2.94	2.47	2.28	1.76	1.61	1.53	2.62	2.13	3.44
K ₂ O	4.35	4.12	3.95	3.63	2.85	2.83	2.59	2.76	2.32
Total	100.00	100.00	100.00	100.00	100.00	100.00	100.01	100.00	100.00

Burney								Aguilera		
	Bu 5-1	Bu 5-10	Bu 5-8	Bu 5-15	Bu 5-16	Bu 5-17	Bu 5-2	Pr 283-3	Pr 283-12	Pr 283-12
SiO ₂	76.03	78.56	75.01	75.86	79.17	76.73	76.44	77.43	77.67	78.20
TiO ₂	0.33	0.39	0.29	0.33	0.34	0.33	0.32	0.41	0.18	0.19
Al ₂ O ₃	14.17	12.17	14.22	13.91	11.93	13.52	13.56	12.51	12.41	12.30
Cr ₂ O ₃	0.00	0.00	0.00	0.00	0.04	0.00	0.00	0.00	0.01	0.01
FeO	0.79	1.26	1.42	1.66	1.42	1.20	1.67	1.37	0.58	0.48
MnO	0.03	0.06	0.00	0.04	0.04	0.00	0.01	0.00	0.01	0.01
MgO	0.15	0.35	0.33	0.37	0.14	0.15	0.29	0.09	0.11	0.10
CaO	2.87	1.89	2.45	2.25	1.59	2.24	2.27	1.56	0.83	0.78
Na ₂ O	4.43	3.51	4.41	3.52	3.36	4.21	3.72	3.33	5.73	4.9
K ₂ O	1.19	1.80	1.87	2.06	1.97	1.62	1.72	3.30	2.48	2.99
Total	100.00	100.00	100.00	100.00	100.00	100.00	100.00	100.00	100.00	100.00

CHEMICAL COMPOSITION OF VOLCANIC GLASSES AND TEPHRA ALTERATION

Representative compositions of volcanic glass from various tephra layers of different sediment and peat cores are given in table 2. Since electron microprobe analyses of alkali elements require relatively wide electron beams ($\phi=5-10\ \mu\text{m}$), measurement conditions used in the electron microprobe analysis are often a compromise between optimum conditions and tephra size constraints, and these data may thus represent only an approach to the original glass composition.

Also, alkali loss is a typical phenomenon during glass alteration, depending on the tephra structure and composition as well as on the acidity of the hydrous environment in which the tephra is deposited (Ericson *et al.*, 1976). Typically, for tephra in the cores from Magallanes, the outer 1-5 μm of tephra glass surfaces have often suffered significant alkali loss, and because many of the tephra glass shards

are often only a few micrometers in size, they may have lost alkali elements throughout. This problem may also affect glass in small pumice fragments, which are often vesicle-rich, with glass partitions between the vesicles only 5-10 μm thick.

Glass compositions were measured in tephra of different grain sizes, deposited in various peat and lake sediment cores after the 4254 ± 120 cal. year BP Mount Burney eruption. The results indicate a greater alkali loss in glass from small tephra glass shards in a peaty environment. This results in a pronounced volcanic glass alteration trend (Fig. 5a) which is most pronounced in the acid (pH 3-4.5) ombrogenic parts of the peat core. In the Austral Andes, where peat soils are dominant, accelerated tephra alteration may represent an important nutrient supply for the otherwise generally nutrient-poor soils of the area (Young 1972). In the peat core GC-2, some thin clay-rich tephra layer are partly transformed to siderite and rhodochrosite layers, so that their original chemistry is altered.

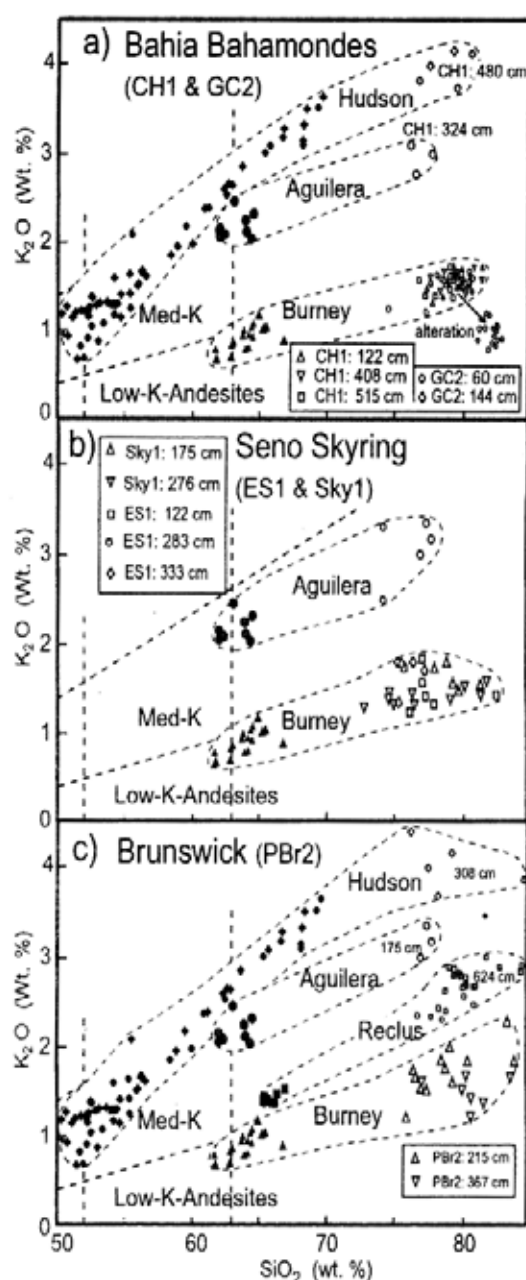


FIG. 5. K_2O versus SiO_2 contents of volcanic glasses from tephra layers (open symbols) at different depths (cm) in various peat and sediment cores (CH1, GC2, ES1, Sky1 and PBr2; Figs. 1, 2, 3) from (a) Gran Campo Nevado area at the main Andean Cordillera; (b) the Skyring area and (c) the Peninsula Brunswick of the southernmost Andes, compared to those of volcanic rocks (solid symbols) from the Aguilera, Reclus and Mount Burney volcanoes in the Andean Austral Volcanic Zone (Stern and Kilian, 1996) and Hudson volcano in the Southern Volcanic Zone (Kilian, 1997; Naranjo and Stern 1998).

Despite these analytical problems, most of the glass compositions of the different layers of tephra found in different cores fit well into the known fractionation trends of the active volcanoes of the southern Andes (Fig. 5; Stern and Kilian, 1996; Kilian, 1997). These tephra glasses generally have a rhyolitic composition. Their K_2O versus SiO_2 content distinguishes their volcanic sources among the different active eruption centers of the southern Andes (Fig. 5). However, the glass composition of different Holocene eruptions from Mount Burney are mutually indistinguishable. Compositions of plagioclase, pyroxene, mica and amphibole phenocrysts in the tephra layers were also determined by the electron microprobe, but their compositions show complex chemical zoning and do not clearly reflect the different possible volcanic sources (Kilian *et al.*, 1991; Stern and Kilian, 1996).

TEPHROCHRONOLOGY

Lithological characteristics, ages (in cal. yr BP) and ash contents (mineral and glass content) of the minerogenic and ombrogenic peat profiles, as well as the sediment and soil profiles, are shown in Figs. 3 and 4. The volcanic eruptions that produced the tephra layers observed in the different cores are described here from the youngest to the oldest.

The ombrogenic peat (GC-1) from the Bahamondes area in central part of the Andean Cordillera (Fig. 1) contains a small tephra layer (Figs. 3 and 4) at around 95 cm depth, which, based on its chemical composition, is derived from the Mount Burney volcano (Fig. 5a). Two ^{14}C ages from below and above this tephra layer give a minimum to maximum age range of 1879 ± 48 to 2213 ± 90 cal. yr BP for this eruption (Fig. 3; Table 1; Biester *et al.*, 2002). The minimum age is from 5 cm above the tephra layer. In this section of the core the yearly peat growth rate was 0.34 mm/year, suggesting that the tephra is 150 yr older than the radiocarbon age. The maximum age was determined on a sample taken 3 cm below the tephra layer. In this section of the core, the yearly peat growth rate is 0.2 mm/yr, suggesting that the tephra is 150 yr younger than the radiocarbon age. This constrains a more precise minimum to maximum age range for this eruption of 2026 ± 48 to 2063 ± 90 cal. yr BP. A tephra layer derived from this eruption of the Mount Burney volcano was also detected in the minerogenic GC-2 peat core, where

another maximum age of 2750 ± 34 cal. yr BP was obtained from 10 cm below the tephra layer (Fig. 3). In the sediment core from lake Chandler (CH-1), this tephra is preserved as a very sharp 2 mm thick tephra fall layer (Figs. 2, 3). In the sediment core from the Seno Skyring (ES-1; Fig. 1), around 60 km to the northeast of the Gran Campo Nevado area and to the east of the Mount Burney volcano, this tephra layer is significantly thicker (2–3 cm; Fig. 3), and the tephra grain size increases from <60 μ m on Peninsula Muñoz Gamero to ~0.5 mm in the Skyring core. These data suggest that the tephra fan from this eruption was distributed predominantly to the northeast of Peninsula Muñoz Gamero. However, this Mount Burney eruption seems to have been only a small Plinian eruption, producing a spatially restricted tephra fall not found at other localities.

A tephra layer with chemical composition indicating that it was derived from an eruption of the Aguilera volcano (Fig. 5b) was observed in the sediment core (ES-1; Fig. 1) from Seno Skyring, but in the Gran Campo Nevado area this tephra occurs only in the lake Chandler sediment core (CH-1; Figs. 1, 3). In the Chandler lake core, this very fine-grained tephra is preserved as a sharply defined layer 1.5 mm thick with. An age from 15 cm below this layer gives a maximum age of 3879 ± 32 cal. yr BP. In the Skyring sediment core (ES-1; Fig. 1) this tephra layer is 1–2 cm thick and the grain size reaches 0.2 mm. These localities represent the southern limit of the distribution of tephra derived from an eruption of the Aguilera volcano $<3596 \pm 230$ cal. yr BP (Stern 1990, 1992, 2000).

All the peat and lake sediment cores from the Peninsula Muñoz Gamero, Skyring fjord and Peninsula Brunswick contain a relatively thick (5–15 cm) Mid-Holocene tephra layer (Figs. 2–4) derived from the Mount Burney volcano as indicated by its glass chemistry (Fig. 5). A minimum age of 3921 ± 27 cal. yr BP from the ombrogenic Skyring peat core (Fig. 4) was determined 7 cm above this tephra layer. Peat accumulation rates of 0.23 mm/year in this peat section suggest that the eruption is ~300 yr older than the ^{14}C age. This calculated minimum age of 4221 ± 27 cal yr BP is in good agreement with the 4254 ± 120 cal. yr BP age obtained by Stern (1992, 2000) and McCulloch and Davies (2001) for this Mid-Holocene eruption of Mount Burney.

The Chandler lake sediment core (CH-1) contains a very thin tephra fall layer (1 mm thick), derived from the Mount Burney volcano, about 24 cm below the 4254 cal. yr BP tephra layer and 17 cm below a

^{14}C age of 4952 ± 11 cal. yr BP. Sedimentation rates of 0.23 mm/year in this section of the sediment core suggests that the small eruption of Mount Burney that produced this layer occurred about 5691 ± 11 cal. yr BP.

The next oldest Holocene tephra layer in the Chandler lake sediment core (CH-1) is derived from the Hudson volcano as indicated by the composition of this glass (Fig. 5a). This tephra also occurs as 1–2 mm thick layer in minerogenic peat core (GC-2; Figs. 1, 3) from Bahamondes at the Gran Campo Nevado area, as well as in the Peninsula Brunswick ombrogenic peat core (Pbr-2; Fig. 4) where this layer is significantly thicker (2–3 cm). ^{14}C ages obtained from above and below this tephra layer in the minerogenic peat core GC-2 give a minimum to maximum age-range of 7705 ± 57 to 8409 ± 17 cal. yr BP. This age range agrees with the minimum age of 6625 ± 110 yr BP ($= 7515 \pm 89$ cal. yr BP) and the maximum age of 6930 ± 120 yr BP ($= 7793 \pm 131$ cal. yr BP) determined by Naranjo and Stern (1998) and improves the minimum age constraint.

An older Holocene tephra derived from another eruption of Mount Burney is observed in the Gran Campo Nevado area as a thin layer (1–2 mm thickness) in both the minerogenic peat core from Bahia Bahamondes (GC-2; Fig. 1c) and the Chandler lake sediment core (CH-1; Figs. 3 and 4). This tephra layer is thicker to the northeast in the Skyring peat core (Sky-1; 2 cm) and still thicker (3–4 cm) towards the southeast in the Brunswick peat core (Pbr-2; Fig. 3). The chemical composition of the glass is indistinguishable from that of other younger Mount Burney tephra layers (Fig. 5; Table 2). A minimum age of 8409 ± 17 cal. yr BP for this tephra was obtained from minerogenic Bahamondes peat core (GC-2; Figs. 1, 3). This age is from 12 cm above the tephra. The peat accumulation rate of 0.2 mm/year in this part of the core section suggests a minimum age of 9009 ± 17 yr for this tephra. A maximum age of 9175 ± 111 cal. yr BP was obtained from directly below this tephra layer in the Chandler lake sediment core (CH-1; Fig. 4). This minimum to maximum age-range of 9009 ± 17 to 9175 ± 111 cal. yr BP gives a more precise time span than the minimum age of 7535 ± 250 ^{14}C yr ($= 8363 \pm 114$ cal yr BP) and maximum age of 8305 ± 250 ^{14}C yr ($= 9271 \pm 215$ cal. yr BP) previously determined by Stern (1992, 2000). The tephra fall of this plinian eruption of Mount Burney was distributed predominantly to the east of the volcano (Fig. 1a).

Two other thin tephra layers derived from Mount Burney occur deeper in the Chandler lake sediment core (CH-1; Fig. 3). The younger of these tephra is dated between 9175 ± 111 and 9511 ± 121 cal. yr BP and the older >9511 cal. yr. BP. Neither tephra layers have been found at other localities and, therefore, these deposits are likely to represent only small eruptions of Mount Burney with limited tephra fans.

A late Pleistocene tephra, with glass composition chemically similar to volcanic products of the Reclus volcano (Fig. 5c), was found in the minerogenic part of the peat core from the Peninsula Brunswick (Pbr-2; Fig. 4). This tephra resulted from the eruption of the Reclus volcano for which a maximum age of 13255 ± 205 yr BP ($=15931 \pm 126$ cal. yr BP) and a minimum age of 12870 ± 200 yr BP ($=15384 \pm 578$ cal. yr BP) has been dated by Stern (1992, 2000). Only this core among those studied provides a record, dating back to this time. The oldest peat core from the Main Andean Cordillera at Bahía Bahamondes near the Gran Camopo Nevado (GC-2; Figs. 1, 3) reaches back to only 14421 ± 612 cal. yr BP and does not contain this Reclus tephra layer.

TEPHRA THICKNESS AND DISTRIBUTION

The tephra layers observed in the cores indicate that Mount Burney had four small and two large Plinian eruptions during the Holocene. The small eruptions produced tephra layers that are either restricted to the Andean area just southeast of the Mount Burney volcano or are difficult to detect in the minerogenic peat cores of the subandean range and terrestrial deposits of the Pampean area to the east.

The eruption fans of the two large Holocene Plinian eruptions of the Mount Burney volcano had different directions. The tephra produced by the older eruption (9009 ± 17 – 9175 ± 111 cal. yr BP) was distributed mainly to the east-southeast of the volcano (Fig. 1a). Our peat and sediment cores from the area south-southeast of Mount Burney all contain this tephra layer, but it is significantly thinner (1–2 mm thickness) in the cores from the Main Andean Cordillera than along the Strait of Magellan near Puerto del Hambre (1–2 cm) and further to the north (>10 cm). In contrast, the younger 4254 ± 120 cal. yr BP large explosive eruption produced a tephra fan which was distributed mainly to the south-southeast

of the volcano (Figs. 1 and 6).

The lake sediment core CH-1 from the Gran Campo Nevado area in the Main Andean Cordillera contains thin tephra layers produced by the large Holocene explosive eruptions of Hudson (7707 ± 185 and 7795 ± 131 cal. yr BP) and Aguilera volcanoes ($<3596 \pm 230$ cal. yr BP), which imply that the southwest edge of the tephra fans from these eruptions reached into the area of the Main Andean Cordillera even far south of these volcanoes (Fig. 1a). This reflects both the very large size of these eruptions, the Hudson eruption being the largest in the southern Andes during the Holocene (Naranjo and Stern, 1998), as well as very unusual southward wind conditions during these eruptions. Such very

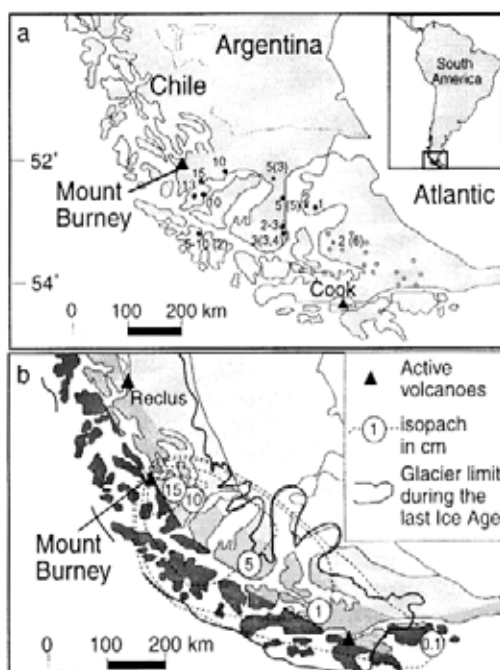


FIG. 6. a- Southernmost Southamerica with investigated localities and tephra thicknesses (numbers indicate thickness in cm) of the 4254 cal. yr BP Mount Burney tephra layer which has been used for an isopach map and tephra volume estimates. Numbers in parentheses indicate references: 1- Auer 1965; 2- Hansen oral communication, 2001; 3- Heusser 1995; 4- Porter *et al.*, 1984; 5- Stern, 1992 and 6- Stern 1990. Filled symbols indicate identified fall deposits of the 4254 Burney eruption. Open circles represent the Tephra III of Auer (1965) which may correspond to this Burney eruption; b- Isopach map (in cm) of the tephra distribution of the 4254 cal. yr BP eruption of the Mount Burney volcano based on the data presented in (a).

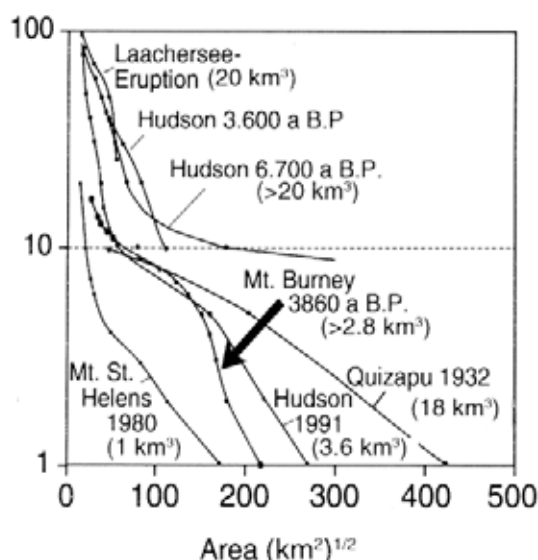


FIG. 7. Tephra thickness versus areas of isopachs for the large Holocene explosive volcanic eruptions of Laachersee (Fisher and Schminke, 1984), Mount Saint Helens (Sarna-Wojcicki *et al.*, 1980), Hudson (Scasso *et al.*, 1994; Naranjo and Stern, 1998) and Quizapu (Hildreth and Drake, 1992), compared to the 4,254 cal. yr BP eruption of Mount Burney. Based on these curves, the tephra volume of the 4,254 cal. yr BP eruption of Mount Burney was calculated as 2.8 km^3 using techniques described by Fierstein and Nathenson (1992).

rare weather conditions occur only in <5 % of all weather situations at the Gran Campo Nevado area (Schneider *et al.*, in press).

THE LARGE MID-HOLOCENE PLINIAN ERUPTION OF THE MOUNT BURNEY VOLCANO

Figure 6 shows locations of occurrences and thicknesses of tephra layers, for the $4,254 \pm 120$ cal. yr BP eruption of Mount Burney volcano, and an isopach map for this eruption based on these data. The tephra thicknesses and areas of isopachs are used to calculate an erupted tephra volume of $2.8 \pm 0.3 \text{ km}^3$ (Fig. 7) after Fierstein and Nathenson (1992). This is approximately half as large as the volume erupted by the Hudson volcano in 1991 ($4\text{--}7 \text{ km}^3$; Naranjo *et al.*, 1993; Scasso *et al.*, 1994), but significantly less than the tephra volume produced by either the 7707 ± 185 and $7,795 \pm 131$ cal. yr BP Hudson eruption ($>18 \text{ km}^3$; Naranjo and Stern, 1998) or the Quizapu eruption in 1932 (18 km^3 ; Larsson, 1936; $\sim 9 \text{ km}^3$; Hildreth and Drake, 1992).

The eruption may have caused the formation of the small summit caldera of the Mount Burney volcano (Fig. 8a). On the eastern and southeastern slopes of Mount Burney, tephra deposits are up to >5 m thick with pumices up to >5 cm in diameter at a distance of 2–3 km from the caldera (Fig. 8b). These tephra deposit continue towards the southeast and the Gran Campo area, and the authors suspect they are the products of the 4254 ± 120 cal. yr BP eruption of Mount Burney volcano.



FIG. 8. (Upper) Satellite image of the Mount Burney volcano showing its summit caldera. (Lower) Holocene tephra deposits, >5 m thick and containing pumices >5 cm in diameter, on the southeastern side of the volcano. These deposits, and possibly the summit caldera, may have been produced by the large explosive eruption at 4254 cal. yr BP, but they have not been dated.

GLOBAL SO₂ PEAKS FROM LARGE SOUTHERN ANDEAN VOLCANIC ERUPTIONS

SO₂ peaks in ice cores from Antarctica can potentially be related to large Plinian eruptions of volcanoes in the southern Andes. The <20,000 yr comprising ice core record of Steig *et al.* (2000) from Taylor Dome, Antarctic, shows significant volcanic derived SO₂ peaks at 3,600 cal yr BP, which may possibly be related to the Aguilera eruption at <3596±230 cal. yr BP, and at 16,000 cal. yr BP, which may be related to the 15384±578 to 15931±126 cal yr BP eruption of Reclus volcano. However, this core does not contain an SO₂ spike in the time period 7707±185 and 7795±131 cal. yr BP

which could corresponds to the very large Mid-Holocene eruption of the Hudson volcano, the largest and most mafic eruption in the southernmost Andes during the Holocene (>20 km³ of tephra; Fig. 8; Naranjo and Stern, 1998), indicating that not all Andean eruptions produced SO₂ peaks in this core.

In contrast to the core record of Steig *et al.* (2000) from Taylor Dome, Antarctica, the 4100 year East-Antarctic ice core record of Cole-Dai *et al.* (2000) does not show a significant SO₂ peaks between 3000 and 4000 cal yr BP. However, at 4100±100 cal yr BP, where the ice core ends, there is a significant SO₂ peak, which possibly could be related to the 4254 cal. yr BP Mount Burney eruption.

ACKNOWLEDGEMENTS

Logistic support during the field work was given by M. Arévalo and G. Cassasa (Universidad de Magallanes, Chile). The authors thank W. Hildreth (U.S. Geological Survey) J.A. Naranjo (Servicio Nacional de Geología y Minería) and C. Heusser

and for constructive comments. German Research Foundation funded grants Ki-456/6-1 and Bi-734/1-1. CS thanks the National Geographic Society for grants to study the tephrochronology of southernmost Patagonia.

REFERENCES

- Auer, V. 1965. The Pleistocene of Fuego-Patagonia Part IV: Bog Profiles. *Annales Academiæ Scientiarum Fennicæ*, Ser. A II, Vol. 80, p. 1-160.
- Auer, V. 1974. The isorhythmicity subsequent to the Fuego-Patagonian and Fennoscandian ocean level transgressions and regression of the last glaciation. *Annales Academiæ Scientiarum Fennicæ*, Ser. A III, Vol. 115, p. 1-188.
- Blester, H.; Kilian, R.; Hertel, C.; Mangini, A.; Shotyk, W.; Scholer, H.-F. 2002. Elevated mercury accumulation in a peat bog of the Magellanic Moorlands, Chile (53°S)- an anthropogenic signal from the Southern Hemisphere. *Earth Planetary Science Letters*, Vol. 201, p. 609-620.
- Blester, H.; Martínez-Cortizas, A.; Birkenstock, S.; Kilian R. 2003. Effect of peat decomposition and mass loss on historic mercury records in peat bogs from Patagonia. *Environmental Science and Technology*, Vol. 37, p. 32-39.
- Cole-Dai, J.; Moseley-Thompson, E.; Wight, S.P.; Thompson, L.G. 2000. A 4100-year record of explosive volcanism from an East Antarctica ice core. *Geophysical Research*, Vol. 105, No. D19, p. 24431-24441.
- Ericson, J.E.; Mackenzie, J.D.; Berger, R. 1976. Physics and chemistry of hydration process in obsidians I: theoretical implication. In *Advances in obsidian glass studies*. (Taylor, R.E.; editor). *Noyes Press*, p. 25-45. Park Ridge.
- Fierstein, J.; Nathenson, M. 1992. Another look at the calculation of fallout Tephra volumes. *Bulletin of Volcanology*, Vol. 54, p. 156-167.
- Fisher, R.V.; Schmincke, H.U. 1984. Pyroclastic flows and rocks. *Springer-Verlag*, 472 p. Berlin.
- Heusser, C.J. 1995. Three Late Quaternary pollen diagrams from Southern Patagonia and their paleoecological implications. *Palaeogeography, Palaeoclimatology, Paleoecology*, Vol. 188, p. 1-24.
- Heusser, C.J. 1998. Deglacial paleoclimate of the American sector of the Southern Ocean: Late Glacial-Holocene records from the latitude of Canal Beagle (55°S), Argentine Tierra del Fuego. *Palaeogeography, Palaeoclimatology, Paleoecology*, Vol. 141, p. 277-301.
- Heusser, C.J.; Heusser, L. E.; Hauser, T.A. 1989-1990. A 12,000 year B.P. tephralayer at Bahía Unutil (Tierra del Fuego, Chile). *Anales del Instituto de la Patagonia*, Vol. 19, p. 39-49.

- Hildreth, W.; Drake, R.E. 1992. Volcán Quizapu, Chilean Andes. *Bulletin of Volcanology*, Vol. 54, p. 93-125.
- Kilian, R. 1997. Magmatismus und Stoffkreislauf an aktiven Kontinentalrändern, untersucht am Beispiel der südlichen Anden. *Zeitschrift der Deutschen Geologischen Gesellschaft*, Vol. 148, No. 1, p. 1-48.
- Kilian, R.; López-Escobar, L.; Lobato, J. 1991. Quaternary volcanism of the Austral Volcanic Zone of the Andes (49-52°S): geochemistry and petrology. In *Symposium on Latin American Geosciences*, No. 12 (Miller, H.; editor et al.). *Zentralblatt für Geologie und Paläontologie*, Part 1, Vol. 1991, No. 6, p. 1709-1721. Stuttgart.
- Kilian, R.; Blester, H.; Maranus, M.; Hohner, M.; Müller, J. 2001. Strong and long-term environmental impact by a Holocene Volcanic eruption in the southernmost Andes. In *Continental margins* (Roth, S.; Rüggeberg, A.; editors). *Schriftenreihe Geologischen Gesellschaft*, Vol. 14, p. 106-107.
- Larsson, W. 1936. Vulkanische Asche vom Ausbruch des chilenischen Vulkans Quizapu (1932) in Argentina gesammelt: eine Studie über Asche-Differentiation. *Bulletin of the Geological Institute of Upsala*, Vol. 26, p. 27-52.
- Markgraf, V. 1993. Younger Dryas in southernmost South America - an update. *Quaternary Science Review*, Vol. 12, p. 351-355.
- Markgraf, V.; Bradbury, J.P.; Schwalb, A.; Burns, J.S.; Stern, C.R.; Ariztegui, D.; Gilli, A.; Anselmetti, F.S.; Stine, S.; Maidana, N. 2003. Holocene Paleoclimates of Southernmost Patagonia: Limnological and Environmental History of Lago Cardiel, Argentina. *The Holocene*, Vol. 13, No. 3, p. 597-607.
- McCulloch, R.D.; Davies, S.J. 2001. Late-glacial and Holocene palaeoenvironmental change in the central Strait of Magellan, southern Patagonia. *Palaeogeology, Palaeoclimate, Palaeoecology*, Vol. 174, p. 143-173.
- McCulloch, R.D.; Bentley, M.J.; Purves, R.S.; Hulton, N.R.J.; Sudgen, D.E.; Clapperton, C.M. 2000. Climatic inferences from glacial and paleoecological evidence at the last glacial termination, southern South America. *Journal of Quaternary Science*, Vol. 15, p. 409-417.
- Naranjo, J.A.; Moreno, H.; Banks, N.G. 1993. La erupción del volcán Hudson 1991 (46°S), Región de Aisén, Chile. *Servicio Nacional de Geología y Minería, Boletín*, Vol. 44, 50 p.
- Naranjo, J.A.; Stern, C.R. 1998. Holocene explosive activity of Hudson volcano, southern Andes. *Bulletin of Volcanology*, Vol. 59, p. 291-306.
- Porter, S.C.; Stuiver, C.M.; Heusser, C.J. 1984. Holocene sea-level changes along the Strait of Magellan and Beagle Channel, Southernmost South America. *Quaternary Research*, Vol. 22, p. 59-67.
- Sahlstein, T.G. 1932. Petrologie der postglazialen vulkanischen Aschen Feuerlands. *Acta Geographica*, Vol. 5, No. 1, p. 4-35.
- Salmi, M. 1941. Die postglazialen Eruptionsschichten Patagoniens und Feuerlands. *Annales Academiæ Scientiarum Fennicæ*, Ser. A III, Vol. 2, p. 1-115.
- Sarna-Wojcicki, A.M.; Shipley, S.; Waitt, R.B.; Dzurisin, D.; Wood, S.H. 1980. Areal distribution, thickness, mass, volume, and grain size of air-fall ash from the six major eruptions of 1980. In *The 1980 eruption of the Mount St. Helens, Washington* (Lipmann, P.W.; Mullineaux, D.R.; editors). *U.S. Geological Survey, Professional Paper*, Vol. 1250, p. 577-600.
- Scasso, R.A.; Corbella, H.; Tiberi, P. 1994. Sedimentological analysis of the tephra from the 12-15 August 1991 eruption of Hudson volcano. *Bulletin of Volcanology*, Vol. 56, p. 121-132.
- Schneider, C.; Glaser, M.; Kilian, R.; Santana, A.; Butorovic, N.; Casassa, G. (In press). Regional Climate Variations across the Southern Andes at 53°S. *Physical Geography*.
- Steig, E.J.; Morse, D.L.; Waddington, E.D.; Stuiver, M.; Grootes, P.M.; Mayewski, P.A.; Twickler, M.S.; Whitlow, 2000. Wisconsinan and Holocene climate history from ice core at Tylor Dome, Western Ross Embayment, Antarctica. *Geografiska Annaler*, Vol. 82, p. 213-235.
- Stern, C.R. 1990. Tephrochronology of southernmost Patagonia. *National Geographic Research*, Vol. 6, p. 110-126.
- Stern, C.R. 1991. Mid-Holocene tephra on Tierra del Fuego (54°S) derived from the Hudson volcano (46°S): evidence for a large explosive eruption. *Revista Geológica de Chile*, Vol. 18, p. 139-146.
- Stern, C.R. 1992. Tefrocronología de Magallanes: nuevos datos e implicaciones. *Anales del Instituto de la Patagonia, Serie Ciencias Naturales*, Vol. 21, p. 129-141. Punta Arenas.
- Stern, C.R. 2000. The Holocene Tephrochronology of southernmost Patagonia and Tierra del Fuego. In *Congreso Geológico Chileno*, No. 9, Actas, Vol. 2, p. 77-80. Puerto Varas.
- Stern, C.R.; Kilian, R. 1996. Role of the subducted slab, mantle wedge and continental crust in the generation of adakites from the Andean Austral Volcanic Zone. *Contributions to Mineralogy and Petrology*, Vol. 123, p. 263-281.
- Stuiver, M.; Reimer, P.J.; Bard, E.; Beck, J.W.; Burr, G.S.W.; Hughen, K.A.; Kromer, B.; McCormac, G.; Van Der Plicht, J.; Spurk, M. 1998. INTACAL98: Radiocarbon Age calibration, 24,000-0 cal. B.P. *Radiocarbon*, Vol. 40, p. 1041-1083.
- Young, S.B. 1972. Subantarctic rain forests of Magellanic Chile: distribution, composition, and age and growth rate studies of common forest trees. *Antarctic Research Series*, Vol. 20, p. 307-322.